AIAA JOURNAL
Vol. 32, No. 4, April 1994

Analysis of Impact of a Moving Body on an Orthotropic Elastic Plate

R. K. Mittal* and M. R. Khalili†
Indian Institute of Technology, New Delhi 110016, India

The problem of transverse impact on large orthotropic elastic plates due to moving impactors is investigated in this paper. The contact force produced during impact is obtained through Sveklo's contact theory for anisotropic bodies. The usual assumption of the contact force being concentrated at a point has been discarded, and instead the elliptical contact region as predicted by the contact theory is considered. The contact force history and the central deflection are only marginally influenced by this replacement as long as the size of the ellipse does not exceed a limit, which for a graphite fiber/epoxy plate of thickness 8 mm is about 1×10^{-4} m; i.e., the size of the ellipse is approximately 1/80 of the plate thickness. However, there is a noticeable effect of a nonzero contact area on the evaluation of the bending curvatures. Also, the well-known singularity in this evaluation is eliminated. The analysis has been illustrated for the case of a graphite fiber-reinforced epoxy plate impacted by steel balls.

I. Introduction

WITH the increasing use of fiber-reinforced composite materials as load bearing structural members, it is essential to understand their response to transverse impact loads for two reasons. Firstly, it is well known that the impact resistance of these materials is poor although the static strength and stiffness in the fiber direction are very good. Secondly, even under low-velocity impact loading, these materials can suffer damage such as internal cracking or delamination. Aircraft structural components where these materials are often used are some times subjected to foreign body impacts such as bird strikes, inadvertent falling of tools during maintenance, etc. These accidental loadings can be very serious and the damage is often invisible. Therefore, a detailed understanding of the dynamic behavior of plates and beams made of aligned fiber-reinforced composites when struck by a moving object is very much needed. For isotropic materials this problem has received adequate attention and the results are well-documented.[1-3] As will be discussed in the next section, this problem is a synthesis of two important problems in the mechanics of solids, viz. the interaction between two bodies in contact and pressing against each other (contact law) and the response of a beam or plate to a known force history. Often this force is assumed to be concentrated at a point.

For two isotropic bodies in contact, Hertz's contact law is generally used. However, when one of the bodies involved in contact is orthotropic as in the case of a compact isotropic body (impactor) striking a fiber-reinforced plate, then Hertz's law needs to be modified or replaced by a law which is also applicable to anisotropic bodies. Various modifications of Hertz's law for transversely isotropic bodies and generally orthotropic bodies have been discussed by Greszczuk.[4] One of the simplest modifications is to replace the expression $E/(1-\nu^2)$ occurring in the case of an isotropic plate by $E_z/(1-\nu_{zr}\nu_{rz})$ for a transversely isotropic plate where E_z is the elastic modulus in the thickness direction (z-axis) and the ν's are the two Poisson's ratios in the r-z plane. This simple modification has been used by some authors[5,6] for an orthotropic plate arguing that $\nu_{zr}\nu_{rz} \simeq 0$, while many investigators have preferred to use a contact law determined from static indentation tests.[7-10] It may, however, be pointed out that the static tests on laminates showed different loading and unloading curves and appropriate power laws were fitted. On the other hand Sveklo's[11] analysis gives a complete description of elastic contact between two anisotropic bodies. Because of its mathematical complexity, it has not been used much except by Frischbier.[12]

As mentioned previously, the contact force is generally assumed to be acting at a point. This leads to a mathematical difficulty, viz. the expressions for bending curvatures become singular[3,12,13] while the use of a nonzero contact area eliminates the singularity.[14] This aspect has been discussed in detail by Khalili[15] and Mittal and Khalili.[16] While some authors have arbitrarily assumed the shape and size of contact area as well as the distribution of the contact force over this area,[8,14] no analysis has been presented so far which considers the actual elliptical contact area as predicted by Hertz's contact theory for isotropic bodies and by Sveklo's theory for anisotropic bodies.

In the present work, Sveklo's analysis has been used to obtain the size and shape of the contact area between an isotropic impactor and an orthotropic plate. The nature of the contact force distribution is also consistent with the contact theory to emphasize a physically realistic situation. The salient features of the contact theory and the expressions for determining the response of a large orthotropic elastic plate will be discussed later. The plate is considered to be large if the fastest flexural waves produced by the impact force do not return, during the time interval of the application of the force, to the point of impact after being reflected at the boundary of the plate. In other words,the reflected waves do not interfere with the impact phenomenon.

II. Basic Equations

Let a large orthotropic plate be subjected to transverse impact as shown in Fig. 1. The axes (x, y, z) are the material coordinates and the origin of the coordinate system is at the center of the contact zone. For a fiber-reinforced plate, the x axis is along the fibers and the y axis is transverse to the fibers in the midplane of the plate. The plate is homogenous and uniformly thick, with thickness h and density ρ. The flexural rigidities of the plate, D_1 and D_2 are defined[17] as

$$D_1 = \frac{E_x h^3}{12(1-\nu_{xy}\nu_{yx})} \tag{1}$$

$$D_2 = \frac{E_y h^3}{12(1-\nu_{yx}\nu_{xy})} \tag{2}$$

Received Jan. 12, 1993; revision received Aug. 17, 1993; accepted for publication Sept. 17, 1993.

*Professor, Department of Applied Mechanics, Hauz Khas.
†Graduate Student; currently Assistant Professor, Faculty of Mechanical Engineering, K. N. T. University of Technology, Tehran, Iran.

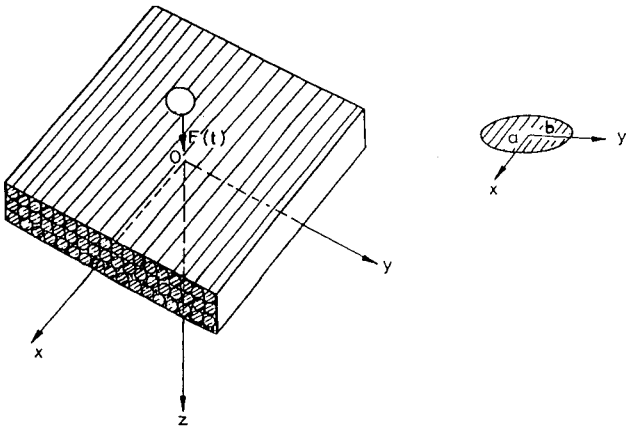

Fig. 1 Elastic orthotropic lamina subjected to a transverse load due to impact; details of the contact area are shown separately.

where E_x and E_y are the elastic modulii of the plate along the fiber direction and transverse to fiber direction, respectively. υ_{xy} and υ_{yx} are the two Poisson's ratios of the plate in the x-y plane. Also, the effective torsional stiffness of the plate D_3 is defined as

$$D_3 = \frac{1}{2}(D_x\upsilon_{yx} + D_y\upsilon_{xy}) + \frac{G_{xy}h^3}{6} \tag{3}$$

where G_{xy} is the shear modulus of the plate in the x-y plane. For the study of the impact behavior of a plate, it is essential to understand the contact phenomenon between two elastic bodies and this is embodied in a contact law. Also, the response of a plate to an applied distribution of transverse force must be known. These two aspects are discussed next.

A. Contact Theory for Two Anisotropic Bodies

Since Sveklo's analysis[11] of contact between two anisotropic bodies shows many features common with Hertz's theory[1,4] of contact for isotropic bodies, we label this analysis as the Hertz-Sveklo contact theory. According to this theory the contact force is distributed over an elliptical region with a and b as semi-axes and the distribution of the contact force is as given below:

$$p(x, y, t) = \frac{3F(t)}{2\pi ab}\left[1 - \frac{x^2}{a^2} - \frac{y^2}{b^2}\right]^{1/2} \tag{4}$$

where $F(t)$ is the total impact force. It may be noted that the contact theories are actually static theories, that is, the applied force is independent of time. However, as pointed out by Rayleigh[18] and others,[1,4,19] these theories are still valid for dynamic situations provided the time of contact is much larger than the time period of the fundamental mode of vibrations of the striker. This is valid if the striker is a small compact mass as compared to the plate.

The impact force $F(t)$ is related to the relative approach, $\delta(t)$ between the striker and the plate through the well-known equation

$$F(t) = K\delta(t)^{3/2} \tag{5}$$

where the constant K is determined from the properties of the striker and the plate. When both the bodies involved in contact are isotropic the expression for the constant K can be easily obtained.[1,4,19] It may also be noted from Hertz's theory that if the impacting bodies are bodies of revolution at least in the neighborhood of the point of contact, then the contact zone is circular with a radius which is proportional to $F^{1/3}$.

Although Eq. (5) is valid for anisotropic bodies also, the expression for K is more complicated than its isotropic counterpart. This is given as follows:

$$K = \frac{4\pi}{3}(1-\epsilon^2)^{3/8}\frac{\left[\int_0^{\pi/2}\sum_{j=1}^{2}\sum_{k=1}^{3}\mathrm{Re}\, i\frac{\Delta_{kj}^{(3)}\Delta_{kj}}{\Delta_{0j}}\frac{d\theta}{(1-\epsilon^2\sin^2\theta)^{3/2}}\right]^{1/2}}{\left[\int_0^{\pi/2}\sum_{j=1}^{2}\sum_{k=1}^{3}\mathrm{Re}\, i\frac{\Delta_{kj}^{(3)}\Delta_{kj}}{\Delta_{0j}}\frac{d\theta}{\Delta}\right]^{3/2}} \times \left[\frac{2R_xR_y}{R_x+R_y}\right]^{1/2} \tag{6}$$

where $i^2 = -1$ and Re represents the real part of the expression and Δ's involve the elastic constants of the two bodies ($j = 1$ or 2) and the roots of two sixth-order polynomial equations. These expressions are available in Refs. 11 and 12. R_x and R_y are defined as

$$\frac{1}{R_x} = \frac{1}{R_{x1}} + \frac{1}{R_{x2}} \tag{7}$$

$$\frac{1}{R_y} = \frac{1}{R_{y1}} + \frac{1}{R_{y2}} \tag{8}$$

where R_{x1} and R_{y1} are the principal radii of the curvature of body 1 in the vicinity of the point of contact while R_{x2} and R_{y2} are the principal radii of curvature for body 2. For the sake of simplicity we consider the case of normal planes containing curvatures $1/R_{x1}$ and $1/R_{x2}$ to be coincident. This is always true if the bodies are spherical or plate-like in the vicinity of the contact point. In this particular case the principal planes can be chosen to contain the direction of fibers reinforcing the plate and the transverse direction.

The other two parameters contained in the expression (6), viz. ϵ and Δ have to be obtained from the following equations:

$$\epsilon^2 = \frac{a^2 - b^2}{a^2} \tag{9}$$

$$\Delta = \sqrt{\frac{a}{b}(1 - \epsilon^2\sin^2\theta)} \tag{10}$$

$$\int_0^{\pi/2}\sum_{j=1}^{2}\sum_{k=1}^{3}\mathrm{Re}\, i\frac{\Delta_{kj}^{(3)}\Delta_{kj}[\cos^2\theta - (R_y/R_x)\sin^2\theta]}{\Delta_{0j}(1-\epsilon^2\sin^2\theta)^{3/2}}\,d\theta = 0 \tag{11}$$

It may be pointed out that from the Eq. (9), ϵ is the eccentricity of the ellipse and is determined by numerically solving Eq. (11). From Eqs. (9) and (10) Δ and a/b are obtained. However, to obtain a and b separately, the contact force F must be known as may be noted from the following equation of Sveklo's analysis:

$$\frac{3}{2\pi}\left(\frac{F}{a^3}\right)\int_0^{\pi/2}\sum_{j=1}^{2}\sum_{k=1}^{3}\mathrm{Re}\, i\frac{\Delta_{kj}^{(3)}\Delta_{kj}}{\Delta_{0j}}\frac{d\theta}{(1-\epsilon^2\sin^2\theta)^{3/2}} = \frac{1}{R_x} + \frac{1}{R_y} \tag{12}$$

Equation (12) shows that for a given pair of impacting bodies, (F/a^3) is constant. Thus a and hence b are proportional to $F^{1/3}$ as in the case of isotropic bodies.

B. Deflection of an Orthotropic Plate due to Transverse Load

For the evaluation of F, it is essential to consider the deflection of the plate. It has been shown by Mittal and Khalili[16] that the deflection of an orthotropic plate due to a transverse load distributed over an elliptical impact area is given by the following equation:

$$w(x, y, t) = \frac{3}{\pi^2\sqrt{\rho h}}\int_0^t F(\tau)\int_0^{\pi/2}\int_0^{\infty}\cos(xp\cos\phi)\cos(yp\sin\phi) \times g(\Lambda)\frac{\sin Ap^2\Phi}{p\Phi}\,dp\,d\phi\,d\tau \tag{13}$$

where

$$A = \frac{t-\tau}{\sqrt{\rho h}} \tag{14}$$

$$\Phi = \sqrt{D_1\cos^4\phi + 2D_3\cos^2\phi\sin^2\phi + D_2\sin^4\phi} \tag{15}$$

$$\Lambda^2 = p^2a^2(1 - \epsilon^2\sin^2\phi) \tag{16}$$

$$g(\Lambda) = \frac{1}{\Lambda^2}\left[\frac{\sin\Lambda}{\Lambda} - \cos\Lambda\right] \tag{17}$$

and

$$\Lambda = pa\sqrt{1 - \epsilon^2\sin^2\phi} \tag{18}$$

The deflection at the center of the ellipse, that is, at $x = 0$, $y = 0$ is given by the following expression:

$$w(0, 0, t) = w_0(t)$$

$$= \frac{3}{\pi^2\sqrt{\rho h}}\int_0^t F(\tau)\int_0^{\pi/2}\int_0^{\infty} g(\Lambda)\frac{\sin Ap^2\Phi}{p\Phi}\,dp\,d\phi\,d\tau \tag{19}$$

This integral can be evaluated numerically for a given total force history $F(\tau)$ and the dimensions a and b of the ellipse. However, if $\Lambda \to 0$ which happens when $a \to 0$, implying that the load is concentrated, then $g(\Lambda) \to \frac{1}{3}$, and the above expression can be evaluated exactly. It has been shown[12] that

$$w_0(t) = \frac{F(\pi/2, \bar{K})}{4\pi\sqrt{\rho h}(D_1D_2)^{1/4}}\int_0^t F(\tau)\,d\tau \tag{20}$$

where $F(\pi/2, \bar{K})$ is the complete elliptic integral of the first kind and

$$\bar{K} = \sqrt{\frac{1}{2} - \frac{(D_3/D_2)}{2\sqrt{D_1/D_2}}} \tag{21}$$

Equation (20) was independently obtained by Olsson (See Appendix in Ref. 5) by a different approach. This equation is the orthotropic counterpart of the expression, obtained by Boussinesq,[20] for the deflection of an isotropic plate subjected to a concentrated transverse load, that is,

$$w_0(t) = \frac{1}{8\sqrt{D\rho h}}\int_0^t F(\tau)\,d\tau \tag{22}$$

where D is the isotropic flexural rigidity. Both equations show that the central deflection is proportional to the impulse imparted to the plate by the striker which is represented by the integral in Eqs. (20) and (22). The constant of proportionality, called the plate parameter (α_p), is the term outside the integral in these equations.

When the load is distributed over a small elliptical region of the plate, instead of being concentrated, the central deflection may depend on the shape and size of the region because of the presence of the $g(\Lambda)$ term in Eq. (13). This dependence has been explored numerically in the next section for a simple load history.

Finally, it also possible to determine the bending and twisting curvatures at any point of the plate. When the load is distributed, the curvature ∂^2w/∂^2x is given as:

$$\frac{\partial^2w(x,y,t)}{\partial x^2} = \frac{-3}{\pi^2\sqrt{\rho h}}\int_0^t F(\tau)\int_0^{\pi/2}[\cos^2\phi]$$

$$\times\int_0^{\infty}\cos(xp\cos\phi)\cos(yp\sin\phi)g(\Lambda)$$

$$\times\frac{\sin Ap^2\Phi}{p\Phi}\,p\,dp\,d\phi\,d\tau \tag{23}$$

For

$$\frac{\partial^2w(x,y,t)}{\partial y^2}$$

and

$$\frac{\partial^2w(x,y,t)}{\partial x\partial y}$$

the term within [ ] is replaced by $\sin^2\phi$ and $\cos\phi\sin\phi$, respectively. At the center of the ellipse the expression (23) can be shown to simplify to the following:

$$\frac{\partial^2w_0(t)}{\partial x^2} = \frac{-6}{\pi^2a^3\sqrt{\rho h}}\int_0^t F(\tau)\int_0^{\pi/2}\frac{\cos^2\phi}{\Phi B^3}\,[\sqrt{\pi A\Phi/2}]$$

$$\times\left[\sin\left(\frac{\pi}{2}z^2\right)C(z) - \cos\left(\frac{\pi}{2}z^2\right)S(z)\right]d\phi\,d\tau \tag{24}$$

where

$$z = \frac{aB}{\sqrt{2\pi A\Phi}}, \qquad B = \sqrt{1 - \epsilon^2\sin^2\phi}$$

Also, C and S are Fresnel's integrals defined as

$$C(z) = \int_0^z \cos\left(\frac{\pi}{2}t^2\right)dt \tag{25}$$

$$S(z) = \int_0^z \sin\left(\frac{\pi}{2}t^2\right)dt \tag{26}$$

The expressions for other curvatures can be written in a similar manner. However, when the load is concentrated the bending curvatures are given by the following simple expressions obtained after some mathematical manipulations:

$$\frac{\partial^2w_0(t)}{\partial x^2} = \beta_x\int_0^t \frac{F(\tau)}{t - \tau}\,d\tau \tag{27}$$

$$\frac{\partial^2w_0(t)}{\partial y^2} = \beta_y\int_0^t \frac{F(\tau)}{t - \tau}\,d\tau \tag{28}$$

where β_x, β_y are the plate parameters for curvatures and are given by the following expressions:

$$\beta_x = \frac{-1}{4\pi}\,[2D_1(\sqrt{D_1D_2} + D_3)]^{-1/2} \tag{29}$$

$$\beta_y = \frac{-1}{4\pi}\,[2D_2(\sqrt{D_1D_2} + D_3)]^{-1/2} \tag{30}$$

The twisting curvature vanishes at the point of load application. For a concentrated load the expressions (27) and (28) for bending curvatures exhibit singularity at $t = \tau$ which implies infinite stresses at the point of loading. This singularity was pointed out by Sneddon[14] for an isotropic plate and Schwieger[3] tried to eliminate it in a semi-empirical way for an isotropic plate. Frischbier[12] adopted same procedure for an orthotropic plate. The nature of the singularity has been studied in detail in a separate publication.[16] However, if the load is not concentrated but distributed over a small region, then the equations of the type (23) are applicable and these exhibit no singularity. In addition, a distributed load is more realistic.

C. Equation for the Determination of Impact Force

The following equation for determining the force history during impact (see, for example Refs. 3 and 13) is well established,

$$\left[\frac{F(t)}{K}\right]^{2/3} = v_0t - \frac{1}{m_s}\int_0^t F(\tau)(t - \tau)\,d\tau - w_0(t) \tag{31}$$

where m_s and v_0 are, respectively, the mass and the striking velocity of the striker. For a concentrated load $w_0(t)$ is given by Eq. (20). However, as mentioned previously, a concentrated load is only an idealization and actually the force is distributed over an elliptical area. Then, $w_0(t)$ is given by Eq. (19). Thus the appropriate equation becomes

$$\left[\frac{F(t)}{K}\right]^{2/3} = v_0t - \frac{1}{m_s}\int_0^t F(\tau)(t - \tau)\,d\tau$$

$$-\frac{3}{\pi^2\sqrt{\rho h}}\int_0^t F(\tau)\int_0^{\pi/2}\int_0^{\infty} g(\Lambda)\times\frac{\sin Ap^2\Phi}{p\Phi}\,dp\,d\phi\,d\tau \tag{32}$$

Not only is this equation more complicated than the equation for the concentrated load, there is one more difficulty. The function $g(\Lambda)$ depends on Λ which is itself a function of the parameter a and ϵ of the ellipse. Also, it was pointed out in Sec. II.A. that a depends on the magnitude of the force since a/F^3 is constant. Let this constant be C. Thus the last integral on the right side of the equation cannot be evaluated numerically before the impact force is known. An alternative to this difficulty is an iterative procedure in which the first approximation of the force history may be obtained by assuming a concentrated load as will be discussed later. Let this be $F^{(1)}(t)$. Using $F^{(1)}(t)$, the first approximation $w_0^{(1)}(t)$ of the central deflection is obtained from Eq. (19). In calculating this, the value of a is modified at each integration step since $a = CF^{1/3}$. Now a modified plate parameter (α_p^*) defined as

$$\alpha_p^* = \frac{w_0^{(1)}(t)}{\int_0^t F^{(1)}(\tau)\, d\tau} \tag{33}$$

is obtained and compared with α_p for the concentrated load. If both differ appreciably, then further iterations are necessary. Fortunately, even for the quite severe cases of impact loading considered by us, α_p^* and α_p differed by less than 0.1%. Thus a concentrated load assumption is justified for the determination of impact force. When the force is assumed to be concentrated, the equation for the determination of impact force can be nondimensionalized to a simple form. Now introduce the following nondimensional quantities:

$$t' = \frac{t}{T_0}, \qquad \tau' = \frac{\tau}{T_0} \tag{34}$$

$$f(t') = \frac{T_0}{m_s v_0} F\left(\frac{t}{T_0}\right) \tag{35}$$

In these expressions T_0 is the reference time given by the following expression:

$$T_0 = \left[\frac{m_s^2}{v_0 K^2}\right]^{1/5} \tag{36}$$

After substituting Eqs. (34–36) into Eq. (31) and simplifying, we obtain the following simple form:

$$f^{2/3}(t') = t' - \int_0^{t'} f(\tau')(t' - \tau')\, d\tau' - \lambda \int_0^{t'} f(\tau')\, d\tau' \tag{37}$$

This integral equation for the determination of impact force depends on a single parameter λ, called the impact parameter. Zener[21] has called it the inelasticity parameter because the impact behavior, particularly the coefficient of restitution, is completely known by it. This parameter is given by the following expression:

$$\lambda = \frac{\alpha_p m_s}{T_0} = \alpha_p (m_s^3 v_0 K^2)^{1/5} \tag{38}$$

Thus if the parameters α_p, m_s, v_0, and K are known for an impact problem, then the history of the impact force is also fully known.

III. Numerical Results and Discussion

To carry out the numerical integration of various equations discussed in the previous section, the data pertaining to a large plate of graphite fiber-reinforced epoxy with 60% by volume of fibers was considered. Such a plate was also considered by Frischbier[12] for his theoretical analysis. He has also reported experimental results for transverse impact with steel balls of various sizes and moving with different velocities. However we have considered only one typical case for numerical analysis. In this case the data for the steel ball are given here: mass $(m_{s1}) = 0.22$ kg, ball radius $(R_{s1}) = 17.7$ mm, and impact velocity $(v_0) = 0.25$ m/s.

The elastic and the other properties of the plate and the ball materials follow:

Plate

$E_x = 123.0$ GPa
$E_y = 9.5$ GPa
$G_{xy} = G_{xz} = 4.7$ GPa
$G_{yz} = 3.2$ GPa
$\upsilon_{zy} = \upsilon_{xz} = 0.3$
$\upsilon_{yx} = \upsilon_{zx} = 0.023$
$\upsilon_{zy} = \upsilon_{yz} = 0.48$

$D_1 = 5284$ Nm
$D_2 = 408$ Nm
$D_3 = 524$ Nm
$\rho = 1515$ kg/m^3
$h = 0.008$ m
$\alpha_p = 10.4 \times 10^{-4}$ m/Ns

Ball

$E_s = 211.0$ GPa
$\upsilon_s = 0.28$
$\rho_s = 7850$ kg/m^3

To determine various parameters dealing with impact, the following step-wise procedure was adopted. First, it is easily noted from Eqs. (7) and (8) that

$$\frac{1}{R_x} = \frac{1}{R_y} = \frac{1}{R_s} \tag{39}$$

because $R_{x1} = R_{y1} = R_s$ and $R_{x2} = R_{y2} = \infty$ where subscripts 1 and 2 refer to the ball and the plate, respectively. Also, from the engineering constants mentioned earlier, the stiffness matrices $(C_{ij})_1$ and $(C_{ij})_2$ for the ball and the plate can be calculated, using the relationships available in textbooks.[17]

First, the evaluation ϵ was taken up using Eq. (11). As $0 \le \theta \le \pi/2$, this interval is divided into n suitable subintervals of size $\Delta\theta$ and for each $\theta = i\Delta\theta$; $(i = 1, 2, 3, \ldots, n)$, the following determinental equation is solved:

$$\begin{bmatrix} C_{11}^* & (C_{12}+C_{66})\cos\theta\sin\theta & \mu(C_{13}+C_{55})\cos\theta \\ (C_{12}+C_{66})\cos\theta\sin\theta & C_{22}^* & \mu(C_{23}+C_{44})\sin\theta \\ \mu(C_{13}+C_{55})\cos\theta & \mu(C_{23}+C_{44})\sin\theta & C_{33}^* \end{bmatrix} = 0 \tag{40}$$

where

$$\begin{aligned} C_{11}^* &= C_{11}\cos^2\theta + C_{66}\sin^2\theta + C_{55}\mu^2 \\ C_{22}^* &= C_{66}\cos^2\theta + C_{22}\sin^2\theta + C_{44}\mu^2 \\ C_{33}^* &= C_{55}\cos^2\theta + C_{44}\sin^2\theta + C_{33}\mu^2 \end{aligned} \tag{41}$$

The preceding equation yields a sixth-order polynomial equation in μ and must be separately solved for the steel ball and the plate. Only even powers of μ occur in the polynomial equation and it is sufficient to consider the roots as μ_1^2, μ_2^2, μ_3^2 which, as shown by Sveklo[11] are either all negative or one of them is negative and the remaining two are complex conjugates of each other.

After the determination of μ's various Δ's are determined, the expressions for which are rather involved and can be obtained from Refs. 11 or 12. Again, these calculations are carried out both for the ball and the plate separately and then substituted into the integral equation (11) to obtain ϵ.

On account of the complexity of these expressions, no direct solution is possible for this integral equation. Therefore, the integral was first evaluated for various values of ϵ^2, both negative and positive, since ϵ^2 is negative if $b > a$. The interval in which the sign of the integral changes is further subdivided. This is continued iteratively until a desired accuracy of ϵ^2 is achieved. In the present example it was found that $\epsilon^2 = -0.41$. Substituting this value of ϵ^2 into Eq. (12), using Eq. (39) and carrying out the numerical integration, the following value is obtained:

$$a/\sqrt[3]{FR_s} = 4.16 \times 10^{-4}\ \text{m/(Nm)}^{1/3}$$

It may be pointed out at this stage that ϵ^2 and $a/(FR_s)^{1/3}$ depend only on the elastic parameters of the ball and the plate. Consequently, on account of Eq. (12), the semi-axes of the ellipse, that is, a and b, are directly proportional to $F^{1/3}$ and $R_s^{1/3}$. These results are of obvious practical significance. Finally, the parameter K is obtained from Eq. (6) and it is easily determined that the quantity $K/(R_s)^{1/2}$ depends only on the elastic properties of the ball and plate. In the present case $K/(R_s)^{1/2} = 1.738 \times 10^{10}$ N/m^2.

Having determined K (because R_s is known), one can proceed with the evaluation of the contact force history and then the deflection and bending curvatures of the plate. However, before carrying out this evaluation, it is useful to investigate the effect of a and ϵ^2 on the central deflection of the plate.

A. Effect of Size and Eccentricity of the Contact Ellipse

To study these effects a rectangular pulse loading as defined hereafter was used:

$$F(t) = \begin{cases} F_0 & \text{for} \quad 0 \le t \le T_c \\ 0 & \text{for} \quad t > T_c \end{cases} \tag{42}$$

First, the effect of a was considered for a fixed value $\epsilon^2 = -0.41$. The value of a was varied from 1×10^{-7} to 0.5×10^{-2} m. The values of $w(x, y, t)$ were found for various points (x, y). However, only one instant of time ($t' = t/T_c = 1.0$) was considered as deflection is maximum at that instant.

The results of numerical integration of Eq. (13) are shown in Fig. 2 after normalization with respect to the deflection obtained for the case of a concentrated load ($a = 0$). This value is known theoretically only at the center ($x = y = 0$),

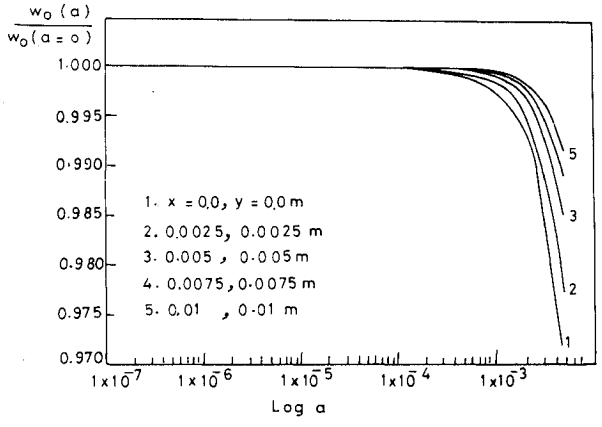

Fig. 2 Effect of contact area size on the deflection of an orthotropic plate at the end of a rectangular pulse load ($t/T_c = 1$).

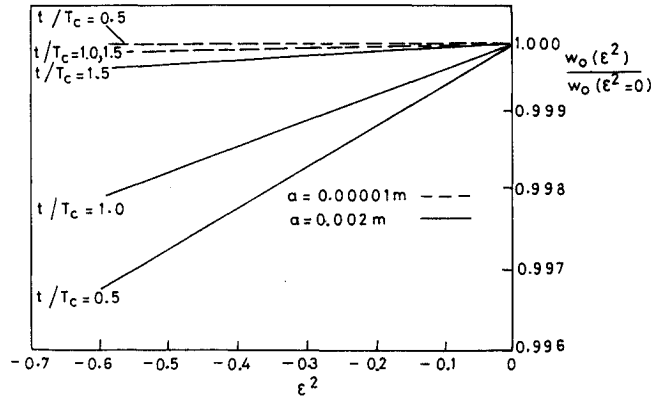

Fig. 3 Influence of the shape of contact area on deflection of an orthotropic plate at the end of a rectangular pulse load for different values of t/T_c.

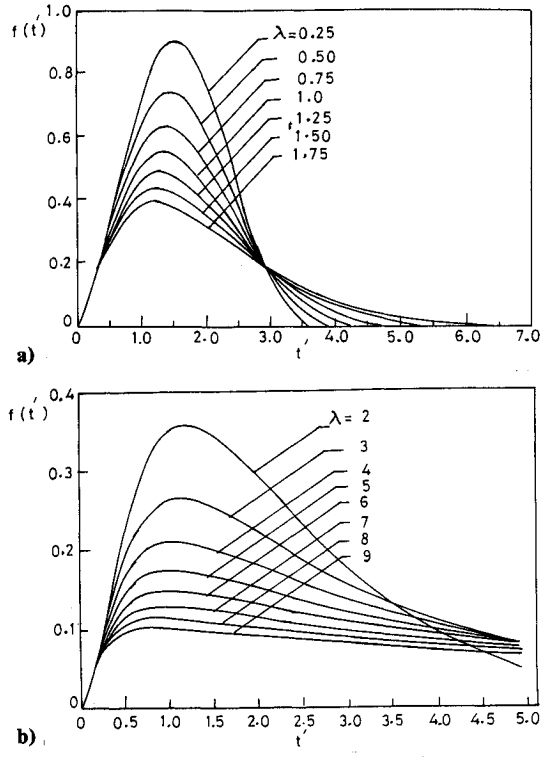

Fig. 4 Variation of dimensionless impact force $f(t')$ with dimensionless time t' for various values of the impact parameter λ: a) $0 < \lambda < 2$ and b) $2 \le \lambda \le 9$.

from Eq. (20). However, it is seen from this figure that for the plate under consideration the deflection at all points remains unchanged when a is less than 1×10^{-4} m or so which was, therefore, used to represent the deflections corresponding to the $a = 0$ case. When the value of a exceeds 1×10^{-4} m there is a rapidly increasing error in the determination of deflection if the actual contact ellipse is replaced by a point. At the center of loading this error is at its maximum and can be around 3% for $a = 5$ mm. Away from the center the magnitude of error decreases.

Next, considering the effect of ϵ^2, it is observed from Fig. 3 that the error involved is negligible even for $a = 0.002$ m. For $a = 1 \times 10^{-5}$ m there is no error. Another point to be noted is that initially ($t/T_c = 0.5$) the effect of eccentricity of the contact region is greater but afterwards the effect is much smaller. In view of this analysis of the roles of a and ϵ^2, a point load can be safely replaced by a distributed load for the purpose of numerical integration such that $a = 1 \times 10^{-6}$ m and $\epsilon^2 = 0.0$, that is, the contact zone is a circle of radius 1 μm.

For any load history $F(t)$ the dynamic response of the plate, i.e., the deflection and the bending curvatures at any point of the plate, can be obtained by integrating Eqs. (13) and (23). These equations are obviously more cumbersome than their concentrated load counterparts (obtained by letting $a = b = 0$ and $g(\Lambda) = 1/3$). To check the validity of the numerical solution it is necessary to compare it with the analytical solution when the latter is available. One such case is that of an isotropic plate for which $D_1 = D_2 = D_3 = D$ where D is the flexural rigidity of the plate.

For the isotropic plate subjected to a concentrated load, exact expressions have been obtained for the deflection and bending curvatures of the plate.[16] In the same paper, a comparison has been made between the deflection at any point using Eq. (13) with $a = 1 \times 10^{-6}$ m, and that obtained by the exact solution assuming a concentrated load. The agreement between the numerical solution and the exact solution was found to be very good at all points of the plate. On the other hand, such a comparison for bending curvatures was satisfactory everywhere except under the point of loading. This is due

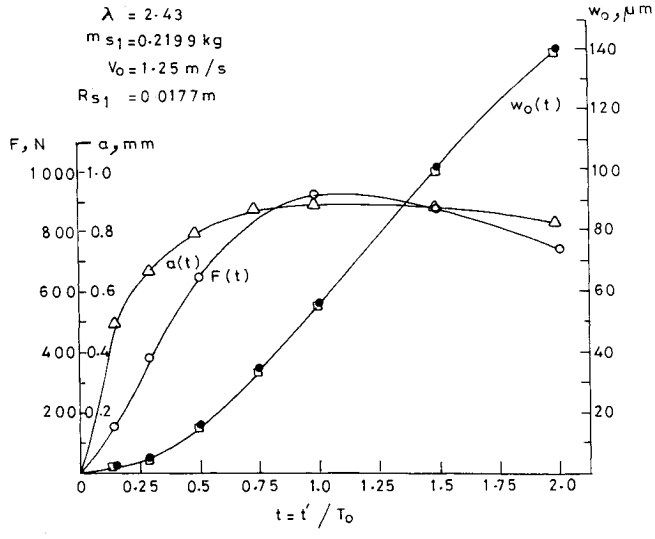

Fig. 5 Variation of impact force history $F(t)$, size of contact ellipse $a(t)$, and deflection of the center of the ellipse $w_0(t)$ with dimensionless time t'; for $w_0(t)$, (•) represents the case $a = 1 \times 10^{-6}$ m while (□) represents the actual size of the contact area.

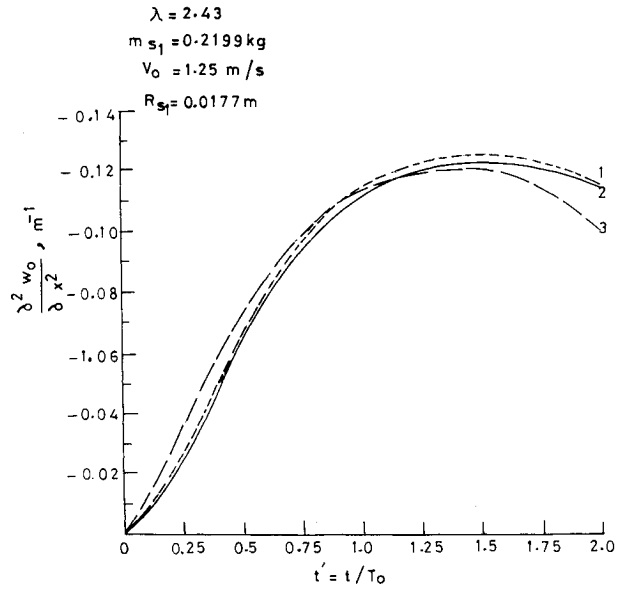

Fig. 6 Variation of central bending curvature $\partial^2 w_0/\partial x^2$ with dimensionless time t'; curve 1: $a = 1 \times 10^{-6}$ m, curve 2: actual contact area, and curve 3: values based on Schwieger's semi-empirical approach.

to the presence of a singularity in the exact solution for bending curvatures at $x = 0$ and $y = 0$, which has been discussed earlier. To overcome the singularity, Schwieger's semi-empirical method was used. This resulted in an error of approximately 8%. Details of these calculations are available in Ref. 16. Finally, it may be stated that the numerical procedure for the integration of Eqs. (13) and (23) yields quite accurate values of the dynamic response functions of an orthotropic plate and is applicable at all points, even for a concentrated load which is simulated by a circle of radius = 1 μm.

B. Determination of Contact Force

After having determined the values of ϵ^2, $K(R_s)^{-1/2}$, and $a(FR_s)^{-1/3}$ for the contact problem, and having established that the appropriate value of a must be used for further analysis, the history of the contact force can be obtained by the solution of the nonlinear integral equation (31). As mentioned in Sec. II.C., instead of solving this equation directly, we first consider Eq. (37), which is the nondimensional counterpart for a concentrated load. The solution can be carried out by Timoshenko's step-by-step method[22] in which Eq. (37) is replaced by the following nonlinear algebraic equation:

$$f_n = (\Delta t')^{3/2}\left[n - \sum_{j=1}^{n} \Delta t' f_j (n-j) - \lambda \sum_{j=1}^{n} f_j \right]^{3/2} \tag{43}$$

where $\Delta t'$ is a suitably small, dimensionless time interval. In each time interval the dimensionless force is assumed to be constant such that $f_j = f(j\Delta t')$. Also, the initial condition is $f_0 = 0$, that is, just at the begining of the contact, the contact force is zero. The solution of Eq. (43) is carried out by an iteration procedure, the details of which can be obtained from several sources.[6,15] Since the solution depends only on parameter λ, the dimensionless force variations were obtained for $0 \le \lambda \le 9$ as shown in Fig. 4. From these curves, the actual impact force curve is obtained as

$$F(t/T_0) = K(v_0 T_0)^{3/2} f(t') \tag{44}$$

Once $F(t)$ is known, the value of a is also known as a function of time since $a/F^{1/3}$ = constant. Then substituting these values in the deflection equation (13), we obtain the central deflection of the plate as a function of time. In Fig. 5, the following computed results are shown for the case of $\lambda = 2.43$: impact force history, $F(t)$; variation of the size of contact ellipse, $a(t)$; and the deflection of the center of the ellipse, $w_0(t)$.

For the determination of $w_0(t)$, two types of calculations were carried out, viz. when $a = 1 \times 10^{-6}$ m to represent a concentrated load as well as when the actual value of a is considered at every instant of time. Both of these results are quite close to each other. Thus the concentrated load assumption is quite good for the evaluation of central deflection.

However, in the case of the evaluation of the bending curvature, the actual size of the contact area should be considered. Figure 6 shows the computational results for the $a = 1 \times 10^{-6}$ m case as well as those based on the actual value of a. Also, the same figure shows the results using Schwieger's semi-empirical procedure of eliminating singularity at $\tau = t$ in Eq. (27) where the upper limit of the integral has been replaced by $t - t_0$. For orthotropic plates the value of t_0 has been given by Frischbier[12] as

$$t_0 = \frac{ab}{4}\sqrt{\frac{\rho h}{D_3}} \tag{45}$$

Again a and b varied with time because of their dependence on $F(t)$. It was also noted that the convergence of the numerical procedure for bending curvatures is much slower than that for deflections.

IV. Conclusions

The principal objective of the present work, that is, the use of an appropriate contact theory for orthotropic plates struck by moving objects, has been achieved. Using the closed-form solutions reported by the authors in an earlier publication, the dynamic response of such a plate has been obtained without making the usual assumption that the impact is concentrated at a point. In fact, it is possible to consider an elliptical area of contact whose size varies with the magnitude of the contact force, as predicted by the theory. During impact the eccentricity of the ellipse does not change. An iterative procedure has been proposed for the determination of the contact force history in which the first approximation is obtained by the assumption of a concentrated force. However, further iterations for the inclusion of the effect of a nonzero contact area improve the solution only marginally for the cases considered. Major effect of the contact area appears to be in the determination of bending curvatures. The well-known singularity at $\tau = t$ associated with a concentrated load is eliminated without any change in the integral involving time.

It is expected that the present work will be helpful in predicting the impact behavior of fiber-reinforced-plastic lami-

nas. However, for laminates, Sveklo's analysis is not strictly valid since it is based on the results for stresses developed in a homogeneous orthotropic half-space when subjected to force on its free surface. But if the individual laminas in a laminate are of sufficient thickness in comparison with the size of the contact ellipse, then the stress interaction between the impactor and the top lamina is only marginally influenced by the presence of other laminas. This is because of the rapid attenuation of stresses in the thickness direction as shown by Greszczuk.[4] The problem of contact between general laminated or nonhomogeneous bodies (isotropic or anisotropic) has not been solved satisfactorily so far. Either approximate solutions are used or the contact law is obtained experimentally.[7]

In spite of these limitations, the analysis presented here is of practical significance. It may be mentioned that the falling weight test is one of the recommended tests for the mechanical characterization of plastics (unreinforced as well as reinforced). This analysis can provide an improved understanding of the test results.

References

[1]Goldsmith, W., *Impact, The Theory and Physical Behaviour of Colliding Bodies,* Edward Arnold, London, 1960, Chap. IV, pp. 82–137.

[2]Schwieger, H., "Vereinfachte Theorie des elastischen Balkenquer-Stoßes und ihre experimentelle Überprüfung," Konstruktiver Ingenieurbau: Berichte Inst. Konstruktiver Ingenieurbau, Ruhr Univ., Bochum, Germany, Vol. 17, 1973, pp. 25–56.

[3]Schwieger, H., "Vereinfachte Theorie des elastischen Biegestoßes auf eine dünne Platte und ihre experimentelle Überprüfung," *Forschung im Ingenieurwesen,* Vol. 41, No. 4, 1975, pp. 122–132.

[4]Greszczuk, L. B., "Damage in Composite Materials due to Low Velocity Impact," *Impact Dynamics,* edited by J. A. Zukas, T. Nicholas, H. F. Swift, L. B. Greszczuk, and D. R. Curran, Wiley, New York, 1982, pp. 55–94.

[5]Olsson, R., "Impact Response of Orthotropic Composite Plates Predicted from a One-Parameter Differential Equation," *AIAA Journal,* Vol. 30, No. 6, 1992, pp. 1587–1596.

[6]Sun, C. T., and Chattopadhyay, S., "Dynamic Response of Anisotropic Laminated Plates under Initial Stress to Impact of a Mass," *Journal of Applied Mechanics,* Vol. 42, No. 3, 1975, pp. 693–698.

[7]Tan, T. M., and Sun, C. T., "Use of Statical Indentation Laws in the Impact Analysis of Laminated Composite Plates," *Journal of Applied Mechanics,* Vol. 52, No. 1, 1985, pp. 6–12.

[8]Dobyns, A. L., "Analysis of Simply-Supported Orthotropic Plates Subjected to Static and Dynamic Loads," *AIAA Journal,* Vol. 19, No. 5, 1981, pp. 642–650.

[9]Wu, H.-Y. T., and Chang, F.-K., "Transient Dynamic Analysis of Laminated Composite Plates Subjected to Transverse Impact," *Composites and Structures,* Vol. 31, No. 3, 1989, pp. 453–466.

[10]Choi, H. Y., Wu, H.-Y. T., and Chang, F.-K., "A New Approach Toward Understanding Damage Mechanisms and Mechanics of Laminated Composites due to Low-Velocity Impact: Part II—Analysis," *Journal of Composite Materials,* Vol. 25, No. 8, 1991, pp. 1012–1038.

[11]Sveklo, V. A., "Hertz Problem of Compression of Anisotropic Bodies," *Journal of Applied Mathematics and Mechanics,* Vol. 38, No. 6, 1974, pp. 1023–1027.

[12]Frischbier, J., "Theorie der Stoßbelastung orthotroper Platten und ihre experimentelle Überprüfung am Beispiel einer undirektional verstärkten CFK- Verbundplatte," Inst. für Mechanik, Ruhr Univ., Bochum, Germany, Rept. 51, 1987.

[13]Mittal, R. K., Schwieger, H., and Truppat, V., "A Simplified Analysis of Transverse Impact on Clamped Circular Plates," Part I—Theory and Part II—Experimental verification, *Journal of Aeronautical Society of India,* Vol. 28, No. 3, 1976, pp. 265–275, 277–282.

[14]Sneddon, I. N., "The Symmetrical Vibrations of a Thin Elastic Plate," *Proceedings of the Cambridge Philosophical Society,* Vol. 41, No. 1, 1945, pp. 27–43.

[15]Khalili, M. R., "Analysis of the Dynamic Response of Large Orthotropic Elastic Plates to Transverse Impact and its Application to Fiber-reinforced Plates," Ph.D. Thesis, Indian Inst. Technology, New Delhi, India, 1992.

[16]Mittal, R. K., and Khalili, M. R., "Analysis of the Dynamic Response of Large Orthotropic Elastic Plates to Transverse Impact," *ZAMM* (submitted for publication).

[17]Vinson, J. R., and Sierakowski, R. L., *The Behaviour of Structures Composed of Composite Materials,* Martinus Nijhoff Publishers, Dordrecht, The Netherlands, 1987, Chap. 3, pp. 63–100.

[18]Rayleigh, J. W. S., "On the Production of Vibrations by Forces of Relatively Long Duration with Application to the Theory of Collisions," *Philosophical Magazine,* Series 6, Vol. 11, 1906, p. 283.

[19]Timoshenko, S. P., and Goodier, J. N., *Theory of Elasticity,* McGraw-Hill, New York, 1970, p. 383.

[20]Boussinesq, J. N., *Application des Potentiels a l'Etude de l'Equilibre et du Mouvement des Solides Elastiques,* Gauthier-Villars, Paris, 1885, pp. 464–480.

[21]Zener, C., "The Intrinsic Inelasticity of Large Plates," *Physical Review,* Vol. 59, April 1941, pp. 669–673.

[22]Timoshenko, S. P., "Zur Frage nach der Wirkung eines Stoßes auf einen Balken," *Zeitschrift für Mathematik and Physik,* Vol. 62, No. 2, 1913, pp. 198–209.